




Research Paper

Effect of Cattaneo-Christov Heat Flux on Radiative Hydromagnetic Nanofluid Flow between Parallel Plates using Spectral Quasilinearization Method

Mangwiro Magodora^{1,2} , Hiranmoy Mondal³ , Precious Sibanda¹ 

¹ School of Mathematics, Statistics and Computer Science, University of KwaZulu-Natal, Private Bag X01, Scottsville, Pietermaritzburg-3209, South Africa

² DST-NRF Centre of Excellence in Mathematical and Statistical Sciences (CoE-MaSS), University of Zimbabwe, Zimbabwe

³ Department of Mathematics, Brainware University, Barasat, Kolkata-700125, India

Received April 17 2020; Revised June 20 2020; Accepted for publication June 20 2020.

Corresponding author: H. Mondal (hiranmoymondal@yahoo.co.in)

© 2021 Published by Shahid Chamran University of Ahvaz

Abstract. In this paper, we numerically solve the equations for hydromagnetic nanofluid flow past semi-infinite parallel plates where thermal radiation and a chemical reaction are assumed to be present and significant. The objective is to give insights on the important mechanisms that influence the flow of an electrically conducting nanofluid between parallel plates, subject to a homogeneous chemical reaction and thermal radiation. These flows have great significance in industrial and engineering applications. The reduced nonlinear model equations are solved using a Newton based spectral quasilinearization method. The accuracy and convergence of the method is established using error analysis. The changes in the fluid properties with various parameters of interest is demonstrated and discussed. The spectral quasilinearization method was found to be rapidly convergent and accuracy is shown through the computation of solution errors.

Keywords: Cattaneo-Christov; Hydromagnetic flow; Quasilinearization; Chebyshev spectral collocation; Gauss Lobatto grid points.

1. Introduction

A nanofluid consists of a base fluid such as water, kerosene, oil or ethylene glycol and suspensions of nanometer sized particles of average size less than 100nm [45]. The nanoparticles are usually metals or metal oxides with higher thermal conductivities than base fluids. The minute size of nanoparticles has the desirable effect of increasing the surface area, which results in increased thermal conductivity of the fluid. Nanoparticles also play the valuable role of improving the viscosity and diffusivity of the base fluid. Nanofluids have important applications in the cooling of heat engines and microsystems, space vehicles, nanomedicine, materials processing, etc. [16]. For this reason, research studies on the rheology of nanofluids has increased on a massive scale in the last few years.

Recently, Muhammad et al. [32] presented a study of bioconvection in the flow of a Carreau nanofluid containing micro-organisms over a wedge. A study using spherical gold (Au) nanoparticles was given by Quresh et al. [38]. Muhammad et al. [35] presented a Darcy-Forcheimer revised model for a nanofluid flow with convective boundary conditions. Sithole et al. [43] discussed the flow of a couple stress nanofluid in a magneto-porous medium while accounting for a chemical reaction and thermal radiation while Pal and Mondal [17] studied the unsteady natural convective MHD boundary-layer flow with a chemical reaction. Sandeep and Sulochana [32] studied the flow of Jeffrey, Maxwell and Oldroyd-B nanofluids with a non-uniform heat source or sink.

Magnetohydrodynamics (MHD) is concerned with the study of electrically conducting fluids. This category of flows finds applications in, *inter alia*, MHD generators, micro MHD pumps, drug delivery, etc. The effects of a magnetic field on different characteristics of electrically conducting fluids have been discussed by, among others, Pal and Mondal [27] and Takhar et al. [47]. Chamkha et al. [4] studied MHD mixed convection flow in a vertical channel. Other studies on MHD flow can be found in Chamkha [4, 6], Patil et al. [18], Pal and Mondal [37], Mondal et al. [26-28] and many others. Research has shown that in wire drawing, subjecting an electrically conducting fluid to a transverse magnetic field may be used to control the rate of stretching and cooling to achieve desirable properties of the finished product [17].



Gorla and Chamkha [16] investigated convection in flow past a vertical plate in a porous medium saturated with a nanofluid. Reddy et al. [40] investigated nanofluid flow past a flat plate in a porous medium. They reported that the shape of nanoparticles has a marked effect on the rate of heat transfer. Mondal and Sibanda [29] studied entropy generation in Sakiadis nanofluid flow. Their study revealed that entropy generation rises in tandem with increased Reynolds numbers.

MHD viscous nanofluid flow between parallel plates has of late received considerable attention from researchers due to their wide application in science and industry. Such flows occur in food processing industries, polymer manufacturing industries, lubricating machines, hydro-dynamical equipment among many other areas. The pioneering study on such flows was done by Stefan [46].

A study of unsteady squeezing flow and heat transfer in flow between parallel plates was presented by Mustafa et al. [35]. They observed that the Nusselt number diminishes with the radiation parameter and the Hartmann number but appreciates with increases in the squeeze number and the Eckert number. A squeezing flow of a third grade fluid was investigated by Shafiq et al. [42] while Das and Mohammed [8] investigated unsteady squeezing flow subjected to a magnetic field. Dib et al. [10] obtained analytical solutions of the equations that model unsteady squeezing nanofluid flow using the Duan-Rach Approach. Sobamowo and Akinshilo [44] investigated double diffusive magnetohydrodynamic squeezing nanofluid flow passing two parallel disks with temperature jump and slip boundary conditions using the homotopy perturbation method.

Lately, many researchers have used the Cattaneo-Christov model in place of some classical models in the study of heat transport problems. In these models heat transfer between two objects is due to a temperature gradient existing between the objects. However, it has been noted that Fourier's law has some inadequacies in fully accounting for the characteristics of heat transfer.

Hayat et al. [20] and Farooq et al. [15] analyzed models based on Christov heat and mass fluxes in a porous media. Hayat et al. [19] interrogated stretching surface in Christov heat flux. Additional literature on the Cattaneo-Christov model can be found in Hayat [20-21], Mondal and Sibanda [29], Oyelakin [36] and Dogonchi and Ganji [13].

The objective of this work is to determine the characteristics of nanofluid flow and heat transfer using the Christov heat flux law and to solve the transport equations the spectral quasilinearization method (SQLM). The SQLM is an iterative Newton-based method in which nonlinear terms in a differential equation are linearized using a Taylor series expansion. In the last decade, many studies have been published where the SQLM was used to solve boundary value problems in fluid dynamics. This trend is attributed to the fact that the SQLM has been found to be robust and efficient. Indeed, it leads to faster convergence in comparison with many other numerical methods such as the finite difference method, Runge-Kutta method and so on [[30, 43]. Other recent studies that used the SQLM include papers by Alharbey et al. [1], Magodora et al. [24], Motsa et al. [31], and Pal et al. [37].

In Section 2, we describe the configuration and give the equations that model the flow and the associated boundary conditions for the squeezing flow. In section 3 the steps followed in applying the SQLM to solve model equations are given. The results are discussed in section 4 with comparisons to previously published literature. The convergence analysis of the SQLM is given to justify its use and give confidence to the findings in the study. Methods that give a fast rate of convergence are important in saving computer memory, time and precision. The choices of parameter values used is informed by literature and a consideration of engineering and industrial applications.

2. Mathematical Formulation

The two-dimensional incompressible Cattaneo-Christov heat flux model between infinite parallel plates saturated with a nanofluid is considered. The parallel plates are placed at $\pm H(t) = \pm l(1 - \alpha t)^{0.5}$ where l is the position at $t = 0$ and α is the squeezing parameter with dimensions of $1/[time]$. For the values of $\alpha > 0$, the parallel plates are squeezed with velocity $v(t) = dH/dt$ at $t = 1/\alpha$, while for $t < 0$, the plates are pulled apart $K_1(t) = k_0/(1 - \alpha t)$. The nanofluid is assumed to be Newtonian. A homogeneous reaction and the base fluid, having the time-dependent reaction rate, is assumed while a time-dependent magnetic field $B(t) = B_0(1 - \alpha t)^{-0.5}$ is applied across the two parallel plates [13, 35]. The slip velocity is assumed to be negligible. Copper nanoparticles are suspended in water which is the base fluid. The thermal and physical properties of these nanofluids are shown in Table 1. The orientations of the x -axis and the y -axis appear in Fig. 1. The velocity components u and v are oriented in x and y directions, respectively. A heat source is placed between plates as depicted on Fig. 1. In tandem with the above assumptions the model equations for mass conservation, linear momentum conservation, energy conservation and mass diffusion are given as:

$$\frac{\partial u}{\partial x} + \frac{\partial v}{\partial y} = 0 \quad (1)$$

$$\rho_{nf} \left(\frac{\partial u}{\partial t} + u \frac{\partial u}{\partial x} + v \frac{\partial u}{\partial y} \right) = -\frac{\partial P}{\partial x} + \mu_{nf} \left(\frac{\partial^2 u}{\partial x^2} + \frac{\partial^2 u}{\partial y^2} \right) - \sigma_f B^2(t)u, \quad (2)$$

$$\rho_{nf} \left(\frac{\partial v}{\partial t} + u \frac{\partial v}{\partial x} + v \frac{\partial v}{\partial y} \right) = -\frac{\partial P}{\partial y} + \mu_{nf} \left(\frac{\partial^2 v}{\partial x^2} + \frac{\partial^2 v}{\partial y^2} \right), \quad (3)$$

$$(\rho C_p)_{nf} \left(\frac{\partial T}{\partial t} + u \frac{\partial T}{\partial x} + v \frac{\partial T}{\partial y} + \varepsilon \Delta \right) = k_{nf} \left(\frac{\partial^2 T}{\partial x^2} + \frac{\partial^2 T}{\partial y^2} \right) - \frac{\partial q_r}{\partial y} + Q_0 T, \quad (4)$$

$$\frac{\partial C}{\partial t} + u \frac{\partial C}{\partial x} + v \frac{\partial C}{\partial y} = D_b \frac{\partial^2 C}{\partial y^2} + \frac{D_r}{T_\infty} \left(\frac{\partial^2 T}{\partial y^2} \right) + K_1(t)C, \quad (5)$$



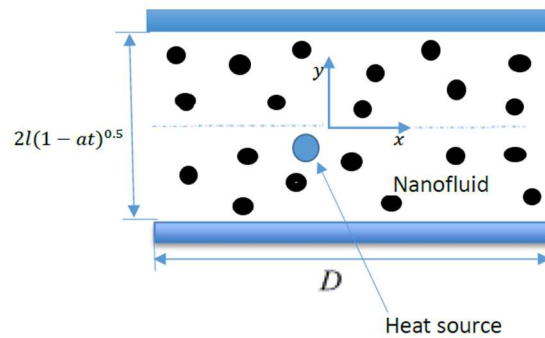


Fig. 1. Flow configuration

where D_T is the thermophoretic diffusion, D_B is the Brownian diffusion, p is the pressure of nanofluid, k_0 is the uniform reaction rate, B_0 is the uniform magnetic field, q_r is the radiative heat flux and:

$$\Delta = \frac{\partial^2 T}{\partial y^2} + \frac{\partial u}{\partial t} \frac{\partial T}{\partial x} + 2u \frac{\partial^2 T}{\partial t \partial x} + 2v \frac{\partial^2 T}{\partial t \partial y} + \frac{\partial v}{\partial t} \frac{\partial T}{\partial y} + u \frac{\partial u}{\partial x} \frac{\partial T}{\partial x} + v \frac{\partial v}{\partial y} \frac{\partial T}{\partial y} + u \frac{\partial v}{\partial x} \frac{\partial T}{\partial y} + v \frac{\partial u}{\partial y} \frac{\partial T}{\partial x} + 2uv \frac{\partial^2 T}{\partial x \partial y} + u^2 \frac{\partial^2 T}{\partial x^2} + v^2 \frac{\partial^2 T}{\partial y^2}. \quad (6)$$

The dynamic viscosity is calculated from the Brinkman model [14] as:

$$\mu_{nf} = \frac{\mu_f}{(1-\varphi)^{2.5}} \quad (7)$$

The other properties of nanofluid are defined as in Rashidi et al. [39]:

$$\rho_{nf} = (1-\varphi)\rho_f + \varphi\rho_s \quad (8)$$

$$(\rho C_p)_{nf} = (1-\varphi)(\rho C_p)_f + \varphi(\rho C_p)_s \quad (9)$$

$$\frac{k_{nf}}{k_f} = \frac{k_s + 2k_f - 2\varphi(k_f - k_s)}{k_s + 2k_f + 2\varphi(k_f - k_s)}. \quad (10)$$

The boundary conditions for the model are (refer to Dogonchi and Ganji [13] and Mustafa et al. [35]):

$$\begin{aligned} u = 0, v = v_w = \frac{dH}{dt}, T = T_H, C = C_H, \text{ at } y = H(t), \\ \frac{\partial u}{\partial y} = v = \frac{\partial C}{\partial y} = \frac{\partial T}{\partial y} = 0 \text{ at } y = 0, \end{aligned} \quad (11)$$

where v_w denotes velocity at the plate surface. By the Roseland approximation, the radiative index q_r is taken as $q_r = -4\sigma^*/3k_{rf}(\partial T^4/\partial y)$ and $T^4 = 4T_\infty^3 T - 3T_\infty^4$. This implies that $\partial q_r/\partial y = -(16/3)(\sigma^* T_\infty^3/k_{rf}^*)\partial T/\partial y$, hence (4) becomes:

$$\frac{\partial T}{\partial t} + u \frac{\partial T}{\partial x} + v \frac{\partial T}{\partial y} + \varepsilon \Delta = \frac{k_{nf}}{(\rho C_p)_{nf}} \left(\frac{\partial^2 T}{\partial x^2} + \frac{\partial^2 T}{\partial y^2} \right) + \frac{16\sigma^* T_\infty^3}{3(\rho C_p)_{nf} k_{nf}^*} \frac{\partial^2 T}{\partial y^2} + \frac{Q_0}{(\rho C_p)_{nf}} T, \quad (12)$$

Let ψ denote the stream function such that $u = \partial\psi/\partial y$ and $v = -\partial\psi/\partial x$, we introduce the following dimensionless variables:

$$\eta = \frac{y}{l\sqrt{1-\alpha t}}, \theta(\eta) = \frac{T}{T_H}, u = \frac{\alpha x}{2(1-\alpha t)} f'(\eta), v = -\frac{\alpha l}{2\sqrt{1-\alpha t}} f(\eta), g(\eta) = \frac{C}{C_H}, \quad (13)$$

Upon effecting the above similarity variables, the model equations and their associated boundary conditions transform to:

$$f^{iv} - \alpha_1 S(3f'' + f'f'' + \eta f''' - f f''') - \alpha_2 M f'' = 0, \quad (14)$$

$$\theta'' + \beta_1 [f\theta' - \eta\theta' - \gamma(\eta^2\theta'' - \eta f'\theta' - 2\eta f\theta'' + ff'\theta' + f^2\theta''')] + \beta_2\theta = 0, \quad (15)$$

$$g'' + ScS(fg' - \eta g') - Sc\zeta g = 0, \quad (16)$$

The boundary conditions are:

$$\begin{aligned} f(0) = 0, f''(0) = 0, \theta'(0) = 0, g'(0) = 0, \\ f(1) = 1, f'(1) = 0, \theta(1) = 1, g(1) = 1, \end{aligned} \quad (17)$$



Table 1. Material properties of base fluid and nanoparticles.

Property	Water (base fluid)	Copper (nanoparticles)
Density, ρ (kgm^{-3})	997.1	893.3
Specific heat capacity, C_p ($\text{Jkg}^{-1}\text{K}^{-1}$)	4179	385
Thermal conductivity, κ ($\text{Wm}^{-1}\text{K}^{-1}$)	0.613	401

where $\alpha_1 = A_1 / A_2$, $\alpha_2 = 1 / A_2$, $\beta_1 = \text{Pr} S A_3 / A_4 (3N / (3N + 4))$, $\beta_2 = (H_s / A_4)(3N / (3N + 4))$. The dimensionless constants A_i for $i = 1, 2, 3, 4$ are defined as $A_1 = \rho_{nf} / \rho_f$, $A_2 = \mu_{nf} / \mu_f$, $A_3 = (\rho C_p)_{nf} / (\rho C_p)_f$ and $A_4 = k_{nf} / k_f$. Here Pr is the Prandtl number, Sc the Schmidt number, S the squeeze number, ζ is the chemical reaction parameter, H_s the heat source parameter, M the magnetic parameter, N the radiation parameter, γ the reaction parameter are defined as:

$$\text{Pr} = \frac{v_f (\rho C_p)_f}{k_f}, \text{Sc} = \frac{v_f}{D_B}, \zeta = \frac{k_0 l^2}{v_f}, S = \frac{\alpha l^2}{2v_f}, H_s = \frac{Q_0 l^2 (1 - \alpha t)}{k_f}, N = \frac{k_{nf} k_{nf}}{4\sigma^* T_\infty^3}, \gamma = \frac{\alpha \varepsilon}{2(1 - \alpha t)}, M = \frac{\sigma_{nf} (1 - \alpha t)^2 B_0^2}{\mu_f}. \quad (18)$$

Physical properties of scientific and engineering interest are the skin friction C_f , the Nusselt number Nu_f and the Sherwood number Sh_f are defined by:

$$C_f \nu_w^2 = \frac{\mu_{nf}}{\rho_f} \frac{\partial u}{\partial y} \Big|_{y=h(t)}, k_f T_H Nu_f = \left(k_{nf} + \frac{16\sigma^* T_\infty}{3k_{nf}} \right) \frac{\partial T}{\partial y} \Big|_{y=h(t)}, Sh_f = -\frac{1}{C_H} \frac{\partial C}{\partial y} \Big|_{y=h(t)} \quad (19)$$

They are deduced from eq. (13) and eq. (19) as:

$$C_f = |A_2 f''(1)|, \quad Nu = \left| A_4 \left(\frac{3N + 4}{3N} \right) \right|, \quad \sqrt{1 - \alpha t} = -g'(1). \quad (20)$$

3. Method of Solution

The method of quasilinearization is used to linearize the nonlinear ordinary differential eq. (14)-(16). Details of this method can be found in Bellman and Kalaba [2]. The iterative scheme that is obtained from applying quasilinearization is:

$$f_{r+1}^{iv} + a_{13r} f_{r+1}''' + a_{12r} f_{r+1}'' - a_{11r} f_{r+1}' + a_{10r} f_{r+1} = R_1 \quad (21)$$

$$a_{21r} f_{r+1}' + a_{20r} f_{r+1} + b_{22r} \theta_{r+1}' + b_{21r} \theta_{r+1}' + b_{20r} \theta_{r+1} = R_2 \quad (22)$$

$$a_{30r} f_{r+1} + g_{r+1}''' + c_{31r} g_{r+1}' - c_{30r} g_{r+1} = R_3, \quad (23)$$

where

$$a_{13r} = \alpha_1 S (f_r - \eta), a_{12r} = \alpha_1 S (3 + f_r) + \alpha_2 M, \quad (24)$$

$$a_{11r} = \alpha_1 S f_r', a_{10r} = \alpha_1 f_r'', \quad (25)$$

$$a_{21r} = \beta_1 \gamma \theta_r' - \beta_1 \gamma f_r \theta_r', a_{20r} = \beta_1 \theta_r' + 2\beta_1 \gamma \eta \theta_r'' - \beta_1 \gamma f_r \theta_r' - 2\beta_1 \gamma f_r \theta_r'', \quad (26)$$

$$b_{22r} = 1 - 1\beta_1 \gamma \eta^2 + 2\beta_1 \gamma \eta f_r - \beta_1 \gamma f_r^2, b_{21r} = \beta_1 f_r - \beta_1 \eta + \beta_1 \gamma \eta f_r' - \beta_1 \gamma f_r f_r', \quad (27)$$

$$b_{20r} = \beta_2, a_{30r} = \text{Sc} S g_r', c_{31r} = \text{Sc} S f_r - \text{Sc} S \eta, c_{30r} = \text{Sc} \zeta, \quad (28)$$

with the boundary conditions are

$$\begin{aligned} f_{r+1}(0) = 0, f_{r+1}'(0) = 0, \theta_{r+1}'(0) = 0, g_{r+1}'(0) = 0, \\ f_{r+1}(1) = 1, f_{r+1}'(1) = 0, \theta_{r+1}(1) = 1, g_{r+1}(1) = 1, \end{aligned} \quad (29)$$

where the subscript r denote the previous approximation while the $r+1$ denotes the current iteration. Further discussion of the quasilinearization method can be found in Magodora et al. [24], Motsa et al. [30], Mondal and Bharti [28] and Mondal and Sibanda [29].

The next step in using the SQLM is to apply the spectral method to the linearized system eq. (23) - (25). Details of the spectral method can be found in Canuto et al. [3], Sithole et al. [43], Pal et al. [37] and Trefethen [48]. The domain of the problem is $\eta \in [0,1]$.



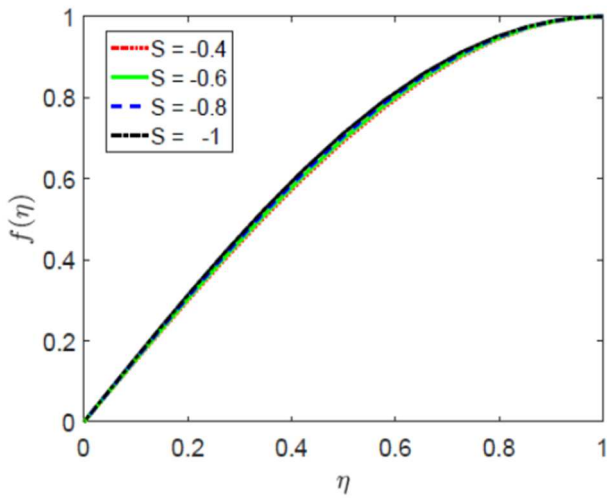


Fig. 2. The impact of squeeze parameter S on nanofluid velocity.

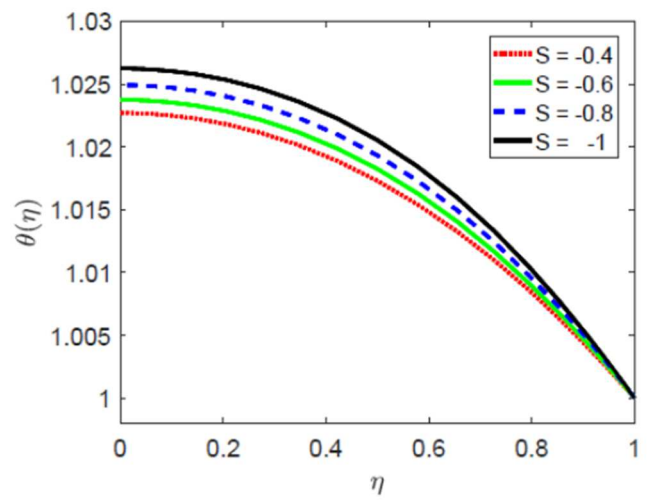


Fig. 3. The impact of squeeze parameter S on temperature.

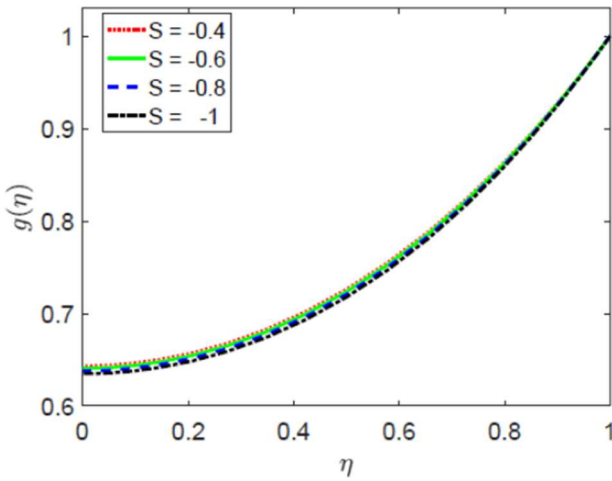


Fig. 4. The impact of squeeze parameter S on concentration of diffusing species.

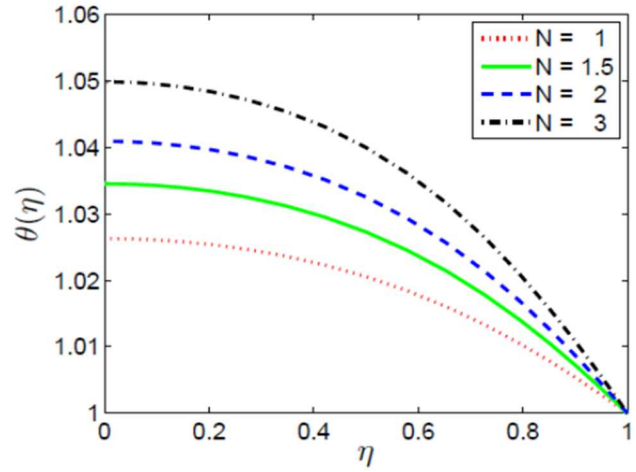


Fig. 5. The impact of the radiation parameter N on temperature.

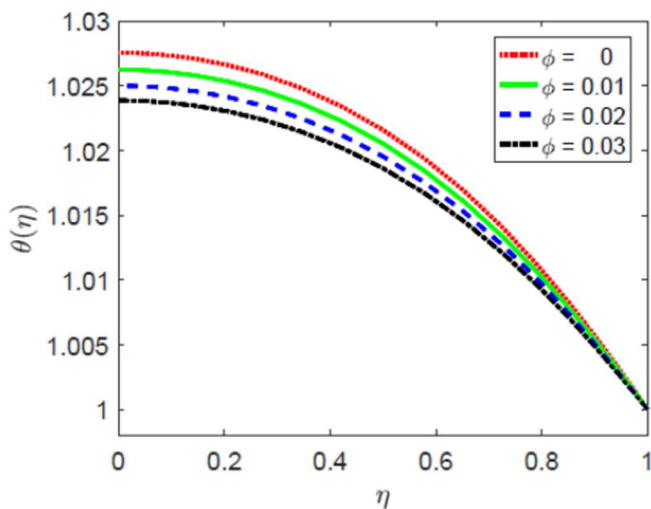


Fig. 6. The impact of solid volume fraction ϕ on temperature.

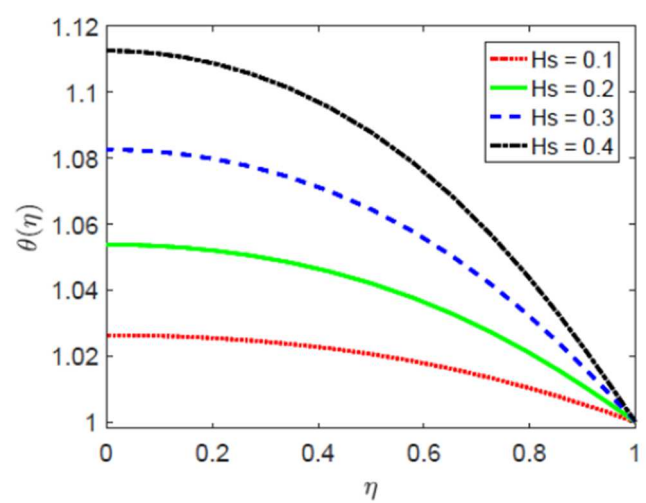


Fig. 7. The impact of heat source parameter H_s on temperature of diffusing species.



To solve the system (22)-(24) with the spectral method, we convert the domain $\eta \in [0,1]$ to $z \in [-1,1]$ by letting $\eta = (z + 1) / 2$. For discretization, we use the Gauss-Lobatto grid points $\eta_i = \cos(\pi i / N)$ for $i = 0, 1, 2, \dots, N$. The derivatives at the Gauss-Lobatto nodes are calculated as $df_n / d\eta|_{\eta_i} = \sum_{w=0}^N D_{iw} f_n(\eta_w)$, where D is the Chebyshev differential matrix and $D_{iw} f_n(\eta_w) = d\tau_w(\eta_i) / d\eta$. Higher order derivatives are defined as $d^p f_n / d\eta^p|_{\eta_i} = D^p F_n$ where $D^p F_n = \sum_{w=0}^N D_{iw}^p f_n(\eta_w)$ and $F_n = [f_n(\eta_0), f_n(\eta_1), \dots, f_n(\eta_N)]^T$ and T denotes transpose of the matrix.

The following initial guesses are chosen in such a way that they satisfy the boundary conditions

$$r = -\frac{1}{2}\eta^3 + \frac{3}{2}\eta, \theta = \eta^2, \text{ and } g = \eta^2.$$

Applying spectral method to system (21)-(23) yields

$$A_{11}f_{r+1} + A_{12}\theta_{r+1} + A_{13}g_{r+1} = R_1 \tag{30}$$

$$A_{21}f_{r+1} + A_{22}\theta_{r+1} + A_{23}g_{r+1} = R_2 \tag{31}$$

$$A_{31}f_{r+1} + A_{32}\theta_{r+1} + A_{33}g_{r+1} = R_3 \tag{32}$$

The boundary conditions for f, θ, g and their derivatives are imposed on the first row, second row, second last row or last row of the square matrices A_{11}, A_{22} and A_{33} as illustrated by Sithole et al. [43]. The linear system $AY=R$ is then solved using MATLAB code where

$$A = \begin{pmatrix} A_{11} & A_{12} & A_{13} \\ A_{21} & A_{22} & A_{23} \\ A_{31} & A_{32} & A_{33} \end{pmatrix}, Y = [f_{r+1} \theta_{r+1} g_{r+1}]^T, R = [R_1 R_2 R_3]^T \tag{33}$$

4. Results and Discussion

The study used the spectral quasilinearization method to investigate the momentum, thermal and concentration properties of a hydromagnetic flow of copper nanofluid between parallel plates in the presence of a homogeneous chemical reaction and thermal radiation. The validity of our methodology and accuracy of results is demonstrated in Table 2 by comparison with previously published results. Excellent agreement is observed.

To show the convergence of the numerical scheme, we computed the solution errors in f, θ, g respectively. The solution errors give the differences between successive iterations, as defined by the norms above. The solution errors are shown in Figs. 13-15 and it is observed that they all reduce, to the order of 10^{-12} after a few iterations, thereby demonstrating fast convergence of the numerical scheme.

The different profiles when the parameters $S, M, \varphi, \gamma, N, H_s, Sc$ and ζ are varied are shown in Figs. 2-11. For the purpose of our numerical simulation we have used the values of $S = 1, M = 1, \varphi = 0.01, Pr = 1, Sc = 1, \gamma = 0.1, N = 1, H_s = 0.1$ and $\zeta = 1$ unless otherwise stated. When a particular parameter is varied, all other parameters are taken to be constant.

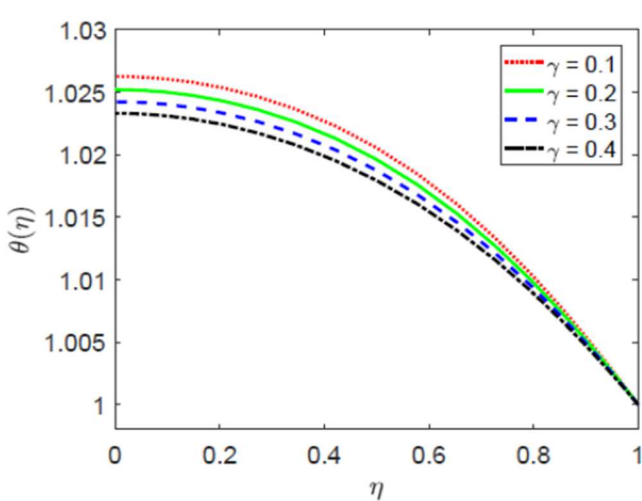


Fig. 8. The impact of the relaxation parameter γ on temperature.

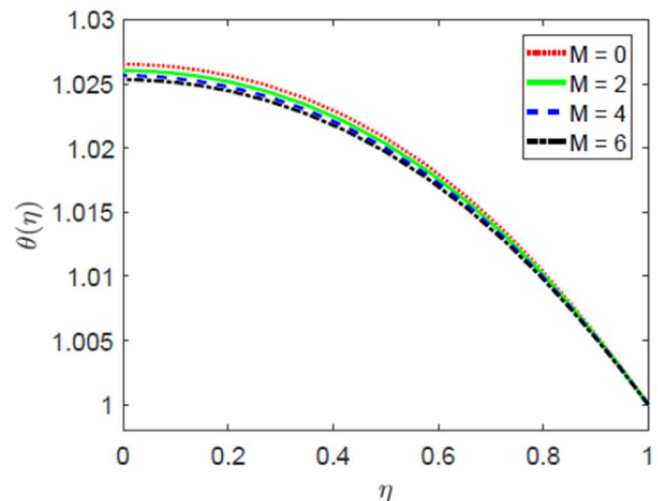


Fig. 9. The impact of magnetic parameter M on temperature.



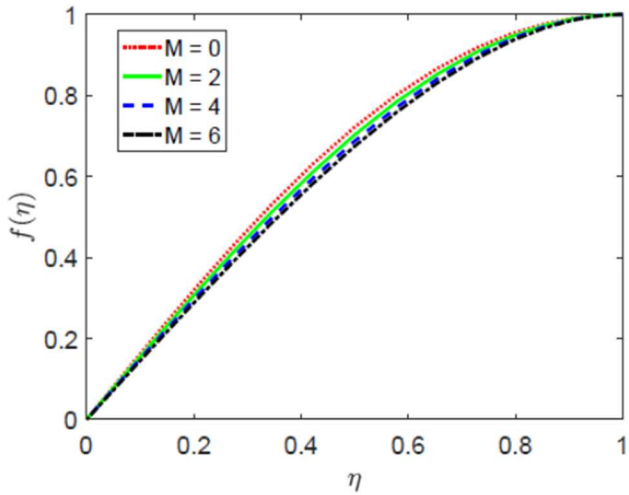


Fig. 10. The impact magnetic parameter M on velocity.

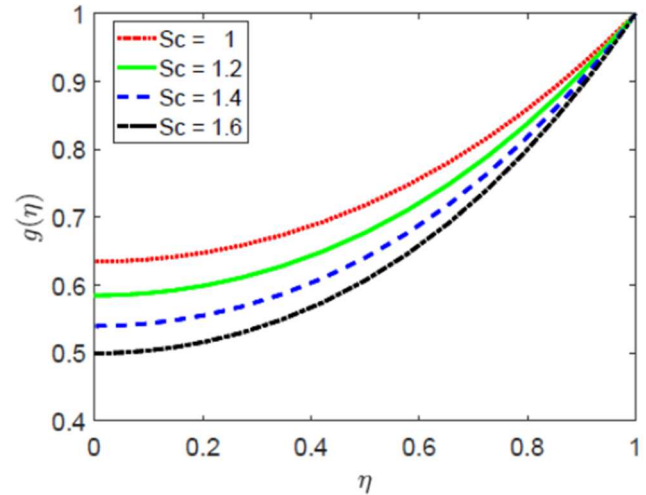


Fig. 11. The impact of the Schmidt number Sc on concentration.

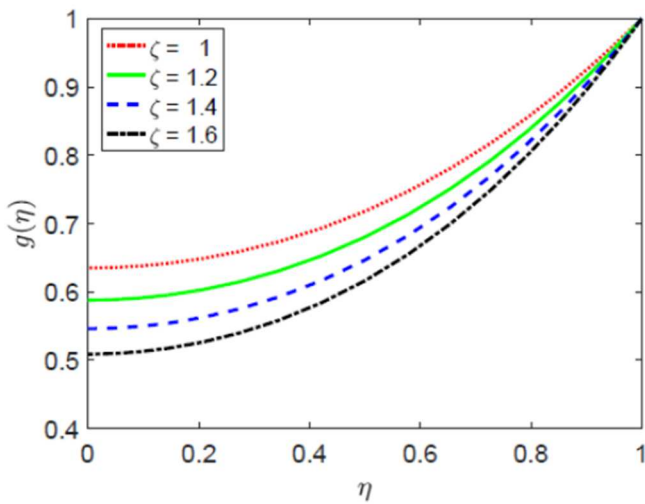


Fig. 12. The impact of chemical reaction parameter ζ on concentration.

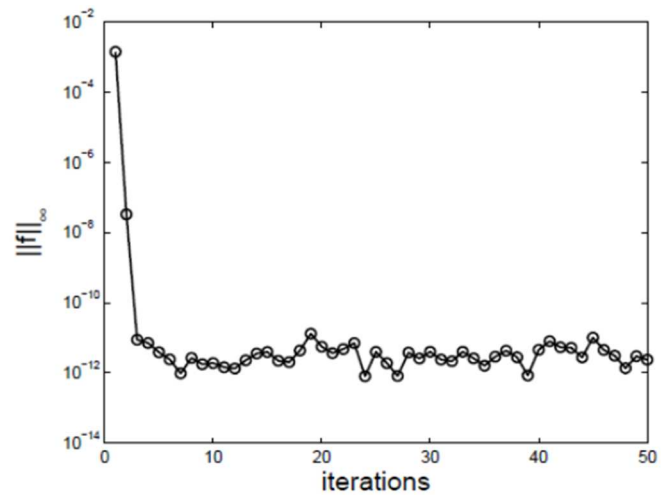


Fig. 13. Solution error for f when $S = -0.3, \phi = 0.01, M = 0.1, Sc = 1$ and $\zeta = 1$.

Figs. 2-4 indicate the influence of the squeezing parameter S , on the various profiles. A downward variation of the squeezing parameter is associated with increased momentum and thermal boundary layers, while the opposite is true for the concentration boundary layer. We considered only negative values of S which correspond to squeezing flow where the plates move towards each other. This action squeezes out the nanofluid and enhances the fluid velocity. Coupled with a greater surface area of the nanoparticles, increased velocity implies enhanced kinetic energy of the nanofluid. This in turn leads to higher thermal conductivity in the nanofluid, hence the increased temperature profiles. It is also apparent that the increased reaction rate causes the species diffusion to reduce significantly due to enhanced velocity and temperature of nanofluid.

The influence of the radiation parameter N on the temperature profiles is shown in Fig. 5 where an increase in radiation leads to an increase in the temperature. As expected, this rise in the temperature increases the Nusselt number as shown in Table 3. It is assumed there is no velocity slip, and as a consequence, Fig. 6 shows that an increase in the volume fraction ϕ , reduces the fluid temperature profiles. The volume fraction is the volumetric concentration of the nanoparticles in the base fluid. Such a relationship between the volume fraction and the temperature were also obtained by Dongonchi et al. [8].

The temperature profiles when heat source parameter H_s is varied, is illustrated in Fig. 7. It is observed, as would be expected, that the temperature increases with the heat source parameter. The physical interpretation of this scenario is that an increased heat source parameter implies increased heat energy being released into the flow, thereby enhancing the thermal boundary layer thickness.

Figure 8 shows the impact of different values of the relaxation parameter γ , where an increase in γ is accompanied by a diminished thermal boundary layer hence a reduced temperature profile. Figures 9 and 10 show the impact of the magnetic parameter on the thermal and momentum profiles respectively. An increased magnetic field reduces the thermal and momentum boundary layers. Strengthening the magnetic field normal to the flow causes the rise of a Lorenz force, which opposes the flow of the electrically conducting nanofluid.



Table 2. Comparison of skin friction coefficient and local Sherwood number values as squeeze parameter S varies at $x=1$ and when $Sc = 1, Pr = 1, \phi = 0.01, H_s = 0, .$

S	$-f''(1)$			$g'(1)$	
	Mustafa et al. [35]	Dogonchi and Ganji [11]	Present Result	Mustafa et al.[35]	Present Results
2	4.1673389	4.167041	4.1673892	0.7018132	0.7018132
0.5	3.336449	3.336449	3.3364495	0.7442243	0.7442243
0.01	3.007134	3.007133	3.0071338	0.7612252	0.7612252
-0.5	2.614038	2.617403	2.6174038	0.7814023	0.7814023
-1	2.170090	2.170090	2.1700909	0.8045580	0.8045588

Table 3. Effects of certain parameters on skin friction coefficient, local Nusselt and Sherwood numbers.

Parameter	Value	$-f''(1)$	$-\theta'(1)$	$g'(1)$
ϕ	0	2.4244886	0.0595669	0.8030504
	0.01	2.3706990	0.0565725	0.8033708
S	-0.4	2.8912768	0.0465793	0.7768018
	-0.6	2.7288755	0.0494688	0.7850880
γ	0.1	2.3706990	0.0565725	0.8033708
	0.2	2.3706990	0.0540696	0.8033708
M	0	2.1179478	0.0572280	0.8048802
	2	2.6048013	0.0559913	0.8048802
H_s	0.1	2.3706990	0.0565725	0.8033708
	0.2	2.3706990	0.1153963	0.8033708
ζ	1	2.3706990	0.0565725	0.9205214
	1.2	2.3706990	0.0565725	1.1287782

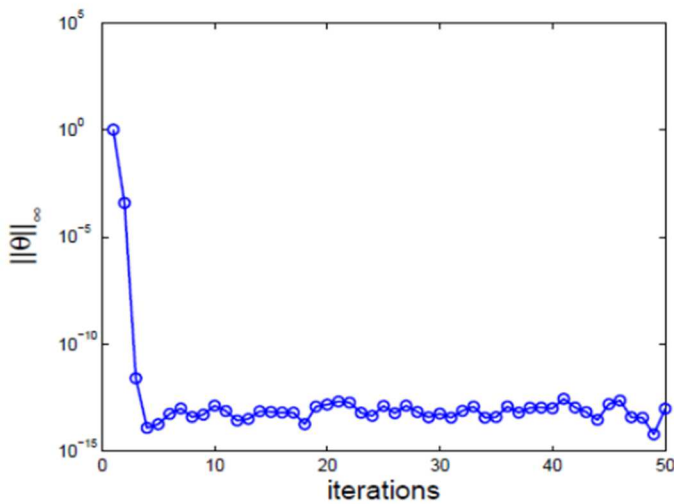


Fig. 14. Solution error for θ when $S = -0.3, \phi = 0.01, M = 0.1, Sc = 1$ and $\zeta = 1$.

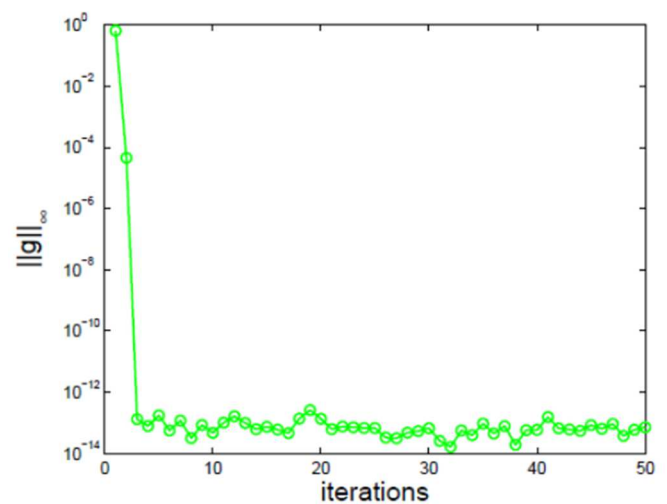


Fig. 15. Solution error for g when $S = -0.3, \phi = 0.01, M = 0.1, Sc = 1$, and $\zeta = 1$.

The effect of different values of Schmidt number on the species concentration profiles is shown in Fig. 11. The Schmidt number is a ratio of mass diffusion to momentum diffusion. It is noted that reduced molecular activity occurs due to increased Schmidt number. The influence of the chemical reaction parameter ζ on the species concentration is portrayed in Fig. 12. It is noticeable that an increased chemical reaction parameter leads to increased chemical reaction, which consequently leads to decreased concentration of the diffusing species, as expected. Table 3 shows the effects of varying the parameter S, M, ϕ, γ, H_s and ζ on $-f''(1), \theta'(1)$ and $g'(1)$. It is apparent that an increase in the magnetic parameter M is associated with a decrease in $\theta'(1)$ and $g'(1)$ but is accompanied by an increase in $-f''(1)$.

5. Conclusion

The study considered heat and mass transfer in an electrically conducting nanofluid between parallel plates with radiation, homogeneous chemical reaction and a magnetic field that is transverse to the flow. The model equations were solved numerically using the spectral quasilinearization method. The accuracy of the method was shown through convergence analysis and by comparing current results with published results in the literature, excellent agreement was established. This study illustrates the efficiency and precision of the spectral quasilinearization method in solving nonlinear flow problems. The impact of the Schmidt number Sc , the relaxation parameter γ , the squeeze parameter S , the solid volume fraction ϕ , the radiation parameter N , the heat source parameter H_s , the magnetic parameter M and the chemical reaction parameter ζ on the skin friction coefficient, Nusselt number, Sherwood number, velocity, temperature and concentration profiles was examined and the results discussed in detail. Highlights of the results from the study are that:



1. An increase in the magnetic parameter leads to a decrease in the local Nusselt and Sherwood numbers but is accompanied by an increase in the skin friction coefficient.
2. An increase in the volume fraction acts to reduce the Sherwood numbers.
3. The temperature decreased with the relaxation parameter and increased with the heat source parameter.

Author Contributions

The manuscript was written through the contribution of all authors. All authors discussed the results, reviewed and approved the final version of the manuscript.

Acknowledgement

The authors are grateful for the financial support rendered by the University of KwaZulu-Natal and the DST-NRF Centre of Excellence in Mathematical and Statistical Sciences (CoE-MaSS).

Conflict of Interest

The authors declared no potential conflicts of interest with respect to the research, authorship and publication of this article.

Funding

The authors received no financial support for the research, authorship, and publication of this article.

Data Availability Statements

The datasets generated and/or analyzed during the current study are available from the corresponding author on reasonable request.

Nomenclature

A_i	dimensionless constants, where $i = 1, 2, 3, 4$	Sc	Schmidt number
$B(t)$	variable magnetic field	$SQLM$	spectral quasilinearization method
B_0	uniform magnetic field	T	temperature (K)
C	concentration (mol/m^3)	T_H	temperature of plate (K)
C_H	concentration at plate surface (mol/m^3)	T_∞	free stream temperature (K)
C_∞	free stream concentration (mol/m^3)	<i>Greek letters</i>	
C_p	specific heat capacity ($Jkg^{-1}K^{-1}$)	α	squeeze rate (s^{-1})
D_B	Brownian diffusion	η	dimensionless variable
D_T	thermophoretic diffusion	ρ	density (kgm^{-3})
f	dimensionless velocity	φ	volume fraction of nanoparticles
g	dimensionless concentration	Θ	dimensionless temperature
H_s	heat source parameter	σ	electrical conductivity (Ωm)
k	thermal conductivity ($Wm^{-1}K^{-1}$)	σ^*	Stefan-Boltzmann constant
k_0	uniform reaction rate	μ	dynamic viscosity (Nsm^{-2})
k^*	mean absorption coefficient	ν	kinematic viscosity (m^2s^{-1})
$K_i(t)$	time - dependent reaction rate	γ	reaction parameter
M	magnetic parameter	ζ	chemical reaction parameter
N	radiation parameter	<i>Subscripts</i>	
Pr	Prandtl number	f	base fluid
q_r	radiative heat flux	nf	nanofluid
S	squeeze parameter		


References


- [1] Alharbey, R.A., Mondal, H., Behl, R., Spectral Quasilinearization Method for Non-Darcy Porous Medium with Convective Boundary Condition, *Entropy*, 21(9), 2019, 838-850.
- [2] Bellman, R.E., Kalaba, R.E., *Quasilinearization and nonlinear boundary-value problems*, American Elsevier Pub. Co., New York, 1965.
- [3] Canuto, C., Hussaini, M.Y., Quarteroni, A., Thomas Jr, A., *Spectral methods in fluid dynamics*, Springer-Verlag, Heidelberg, 1988.
- [4] Chamkha, A.J., On laminar hydromagnetic mixed convection flow in a vertical channel with symmetric and asymmetric wall heating conditions, *International Journal of Heat and Mass Transfer*, 45(12), 2002, 2509-2525.
- [5] Chamkha, A.J., Takhar, H.S., Soundalgekar, V.M., Radiation effects on free convection flow past a semi-infinite vertical plate with mass transfer, *Chemical Engineering Journal*, 84(3), 2001, 335-342.
- [6] Chamkha, A.J., Nath, G., MHD flow over a moving plate in a rotating fluid with magnetic field, Hall currents and free stream velocity, *International Journal of Engineering Science*, 40(13), 2002, 1511-1527
- [7] Daniel, Y.S., Aziz, Z.A., Ismail, Z., Salah, F., Entropy analysis in electrical magnetohydrodynamic (MHD) flow of nanofluid with effects of thermal radiation, viscous dissipation, and chemical reaction, *Theoretical and Applied Mechanics Letters*, 7(4), 2017, 235-242.
- [8] Das, K., Mohammed, U., Radiation effects on an unsteady squeezing flow in the presence of a magnetic field, *Moldavian Journal of the Physical Sciences*, 15(1-2), 2002, 101-110.
- [9] De, P., Mondal, H., Bera, U.K., Heat and Mass Transfer in a Hydromagnetic Nanofluid Past a Non-Linear Stretching Surface with Thermal Radiation, *Journal of Nanofluids*, 4(2), 2015, 230-238.




- [10] Dib, A., Haiahem, A., Bou-Said, B., Approximate analytical solution of squeezing unsteady nanofluid flow, *Powder Technology*, 269, 2015, 193-199.
- [11] Dogonchi, A.S., Divsalar, K., Ganji, D.D., Flow and heat transfer of MHD nanofluid between parallel plates in the presence of thermal radiation, *Computer Methods in Applied Mechanics and Engineering*, 310, 2016, 58-76.
- [12] Dogonchi A.S., Ganji D.D., Investigation of MHD nanofluid flow and heat transfer in a stretching/shrinking convergent/divergent channel considering thermal radiation, *Journal of Molecular Liquids*, 220, 2016, 592-603.
- [13] Dogonchi, A.S., Ganji, D.D., Impact of Cattaneo-Christov heat flux on MHD nanofluid flow and heat transfer between parallel plates considering thermal radiation effect, *Journal of the Taiwan Institute of Engineers*, 80, 2017, 52-63
- [14] Fadhilah, S.A., Hidayah, I., Hilwa, M.Z., Faizah, H.N., Marhamah, R.S., Thermophysical properties of Copper/Water nanofluid for automotive cooling system, *Journal of Mechanical Engineering and Technology*, 5(2), 2013, 1-10.
- [15] Farooq, M., Ahmad, S., Javed, M., Anjum, A., Analysis of Cattaneo-Christov heat and mass fluxes in the squeezed flow embedded in porous medium with variable mass diffusivity, *Results in Physics*, 7, 2017, 3788-3796.
- [16] Gorla, R.S.R., Chamkha, A., Natural Convective Boundary Layer Flow Over a Nonisothermal Vertical Plate Embedded in a Porous Medium Saturated With a Nanofluid, *Nanoscale and Microscale Thermophysical Engineering*, 15(2), 2011, 81-94.
- [17] Haroun, N.A., Mondal, S., Sibanda, P., Unsteady natural convective boundary-layer flow of MHD nanofluid over a stretching surfaces with chemical reaction using the spectral relaxation method: A revised model, *Procedia Engineering*, 127, 2015, 18-24.
- [18] Haroun, N.A., Sibanda, P., Mondal, S., Motsa, S.S., On unsteady MHD mixed convection in a nanofluid due to a stretching/shrinking surface with suction/injection using the spectral relaxation method, *Boundary value problems*, 2015, 2015, 24.
- [19] Hayat, T., Farooq, M., Alsaedi, A., Al-Solamy, F., Impact of Cattaneo-Christov heat flux in the flow over a stretching sheet with variable thickness, *AIP Advances*, 5(8), 2015, 087159.
- [20] Hayat, T., Muhammad, K., Farooq, M., Alsaedi, A., Squeezed flow subject to Cattaneo-Christov heat flux and rotating frame, *Journal of Molecular Liquids*, 220, 2016, 216-222.
- [21] Hayat, T., Khan, M.W.A., Alsaedi, A., Ayub, M., Khan, M.I., Stretched flow of Oldroyd-B fluid with Cattaneo-Christov heat flux, *Results in Physics*, 7, 2017, 2470-2476.
- [22] Khan, N.A., Aziz, S., Ullah, S., Entropy generation on MHD flow of Powell-Eyring fluid between radially stretching rotating disk with diffusion-thermo and thermo-diffusion effects, *Acta Mechanica et Automatica*, 11(1), 2017, 20-32.
- [23] Hussain, S.A., Muhammad, S., Ali, G., Shah, S.I.A., Ishaq, M., Shah, Z., Khan, H., Tahir, M., Naeem, M., A Bioconvection Model for Squeezing Flow between Parallel Plates Containing Gyrotactic Microorganisms with Impact of Thermal Radiation and Heat Generation/Absorption, *Journal of Advances in Mathematics and Computer Science*, 27(4), 2018, 1-22
- [24] Magodora, M., Mondal, H., Sibanda, P., Dual solutions of a micropolar nanofluid flow with radiative heat mass transfer over stretching/shrinking sheet using spectral quasilinearization method, *Multidiscipline Modeling in Materials and Structures*, 16(2), 2019, 238-255.
- [25] Mahian, O., Kianifar, A., Kleinstreuer, C., Moh'd, A.A.N., Pop, I., Sahin, A.Z., Wongwises, S., A review of entropy generation in nanofluid flow, *International Journal of Heat and Mass Transfer*, 65, 2013, 514-532.
- [26] Goqo, S., Mondal, H., Sibanda, P., Motsa, S.S., A multivariate spectral quasilinearisation method for entropy generation in a square cavity filled with porous medium saturated by nanofluid, *Case Studies in Thermal Engineering*, 14, 2019, 100415.
- [27] Mondal, H., Almakki, M., Sibanda, P., Dual solution for three-dimensional MHD nanofluid flow with entropy generation, *Journal of Computational Design and Engineering*, 6, 2019, 657-665
- [28] Das, S., Mondal, Kundu, H., Sibanda, P., Spectral quasilinearization method for Casson fluid with homogeneous-heterogeneous reaction in presence of nonlinear thermal radiation over an exponential stretching sheet, *Multidiscipline Modeling in Materials and Structures*, 15(2), 2019, 398-417.
- [29] Mondal, H., Sibanda, P., Spectral Quasi-Linearization Method for Entropy Generation Using the Cattaneo-Christov Heat Flux Model, *International Journal of Computational Methods*, 17(05), 2020, 1940002.
- [30] Motsa, S.S., Dlamini, P.G., Khumalo, M., Spectral relaxation method and spectral quasilinearization method for solving unsteady boundary layer flow problems, *Advances in Mathematical Physics*, 2014, Article ID 341964.
- [31] Motsa, S.S., Sibanda, P., Shateyi, S., On a new quasilinearization method for systems of nonlinear boundary value problems, *Mathematical Methods in the Applied Sciences*, 34(11), 2011, 1406-1413.
- [32] Muhammad, T., Alamri, S.Z., Waqas, H., Habib, D., Ellahi, R., Bioconvection flow of magnetized Carreau nanofluid under the influence of slip over a wedge with motile microorganisms, *Journal of Thermal Analysis and Calorimetry*, 143, 2021, 945-957.
- [33] Muhammad, T., Alsaedi, A., Shehzad, S.A., Hayat, T., A revised model for Darcy-Forchheimer flow of Maxwell nanofluid subject to convective boundary condition, *Chinese Journal of Physics*, 55(3), 2017, 963-976.
- [34] Muhammad, T., Alsaedi, A., Hayat, T., AliShehzad, S., A revised model for Darcy-Forchheimer three-dimensional flow of nanofluid subject to convective boundary condition, *Results in Physics*, 7, 2017, 2791-2797.
- [35] Mustafa, M., Hayat, T., Obaidat, S., On heat and mass transfer in the unsteady squeezing flow between parallel plates, *Meccanica*, 47(7), 2012, 1581-1589.
- [36] Oyelakin, I.S., Mondal, S., Sibanda, P., Cattaneo-Christov Nanofluid Flow and Heat Transfer with Variable Properties Over a Vertical Cone in a Porous Medium, *International Journal of Applied and Computational Mathematics*, 3(1), 2017, 1019-1034.
- [37] Pal, D., Mondal, S., Mondal, H., Entropy generation on MHD Jeffrey nanofluid over a stretching sheet with nonlinear thermal radiation using spectral quasilinearisation method, *International Journal of Ambient Energy*, 2019, <https://doi.org/10.1080/01430750.2019.1614984>.
- [38] Qureshi, M.Z.A., Rubbab, Q., Irshad, S., Ahmad, S., Aqeel, M., Heat and mass transfer analysis of MHD nanofluid flow with radiative heat effects in the presence of spherical Au-metallic nanoparticles, *Nanoscale Research Letters*, 11(1), 2016, 472.
- [39] Rashidi, M.M., Ganesh, N.V., Hakeem, A.A., Ganga, B., Buoyancy effect on MHD flow of nanofluid over a stretching sheet in the presence of thermal radiation, *Journal of Molecular Liquids*, 198, 2014, 234-238.
- [40] Reddy, J.V.R., Sugunamma, V., Sandeep, N., Sulochan, C., Influence of chemical reaction, radiation and rotation on MHD nanofluid flow past a permeable flat plate in porous medium, *Journal of the Nigerian Mathematical Society*, 35, 2016, 48-65.
- [41] Sakiadis, B.C., Boundary layer behavior on continuous solid surfaces: Boundary-layer equations for two-dimensional and axisymmetric flow, *AIChE Journal*, 7(1), 1961, 26-28.
- [42] Shafiq, A., Jabeen, S., Hayat, T., Alsaedi, A., Cattaneo-Christov Heat Flux Model For Squeezed Flow Of Third Grade Fluidm, *Surface Review and Letters*, 24(07), 2017, 1750098.
- [43] Sithole, H., Mondal, H., Goqo, S., Sibanda, P., Motsa, S., Numerical simulation of couple stress nanofluid flow in magneto-porous medium with thermal radiation and a chemical reaction, *Applied Mathematics and Computation*, 339, 2018, 820-836.
- [44] Sobamowo, G.M., Akinshilo, A.T., Double diffusive magnetohydrodynamic squeezing flow of nanofluid between two parallel disks with slip and temperature jump boundary conditions, *Applied and Computational Mechanics*, 11(2), 2017, 167-182.
- [45] Sridhara, V., Satapathy, L.N., Al₂O₃-based nanofluids: A Review, *Nanoscale Research Letters*, 6(1), 2011, 456.
- [46] Stefan M.J., Versuch Über die scheinbare adhesion, *Akademie der Wissenschaften. Math Naturwissenschaftliche*, 69, 1874, 713-721.
- [47] Takhar, H.S., Chamkha, A.J., Nath, G., Unsteady three-dimensional MHD-boundary-layer flow due to the impulsive motion of a stretching surface, *Acta Mechanica*, 146, 2001, 59-71.
- [48] Trefethen, L.N., *Spectral methods in MATLAB*, Volume 10, SIAM, 2000.

ORCID iD

Mangwiro Magodora  <https://orcid.org/0000-0002-0449-2474>

Hiranmoy Mondal  <https://orcid.org/0000-0002-9153-300X>

Precious Sibanda  <https://orcid.org/0000-0003-2115-4642>





© 2022 Shahid Chamran University of Ahvaz, Ahvaz, Iran. This article is an open access article distributed under the terms and conditions of the Creative Commons Attribution-NonCommercial 4.0 International (CC BY-NC 4.0 license) (<http://creativecommons.org/licenses/by-nc/4.0/>).

How to cite this article: Magodora M., Mondal, H., Sibanda P. Effect of Cattaneo-Christov Heat Flux on Radiative Hydromagnetic Nanofluid Flow between Parallel Plates using Spectral Quasilinearization Method, *J. Appl. Comput. Mech.*, 8(3), 2022, 865–875. <https://doi.org/10.22055/JACM.2020.33298.2195>

Publisher's Note Shahid Chamran University of Ahvaz remains neutral with regard to jurisdictional claims in published maps and institutional affiliations.

